SIMULATIONS OF THE EMITTANCE COMPENSATION IN PHOTOINJECTORS AND COMPARISON WITH SPARC MEASUREMENTS

C. Ronsivalle, L. Giannessi, M. Quattromini, ENEA, Frascati (Roma), Italy,
M. Ferrario, L. Ficcadenti, D. Filippetto, V. Fusco, B. Marchetti, M. Migliorati, A. Mostacci,
L. Palumbo, C. Vaccarezza, INFN/LNF, Frascati (Roma), Italy
A. Cianchi, INFN-Roma II, Roma, Italy
A. Bacci, A.R. Rossi, L. Serafini, INFN-Milano, Milano, Italy

Abstract

FEL photoinjectors are based on the emittance compensation process, by which a high brightness beam can be accelerated without degradation. The experimental results obtained in the SPARC facility for which the beam dynamics has been extensively simulated confirm the theoretical predictions. The paper illustrates the most relevant beam dynamics results as well as a comparison between simulations and measurements.

SHORT REVIEW OF EMITTANCE COMPENSATION IN PHOTOINJECTORS

The new generation of linac photoinjectors employs the emittance compensation technique in order to get the high brightness electron beams required for the production of FEL radiation in the range from UV to X-rays.

A typical photoinjector scheme consists in a RF gun provided with a photocathode illuminated by a few picoseconds laser pulse followed by a linac accelerating the electron bunch emitted by the cathode to relativistic energies. As the space charge induced rms emittance growth in the RF gun is partially correlated, it is possible to achieve a decreasing evolution of the rms emittance from the gun exit to the output of the booster.

The emittance compensation is well described theoretically in literature [1, 2]: it is done by locating a solenoid at the exit of the gun followed by a drift space and then properly matching the beam to the following accelerating sections according to the so called "invariant envelope" condition, consisting in injecting the beam at a laminar waist ($\sigma'=0$) in a matched accelerating structure of a linac booster given by

$$\gamma' = \frac{2}{\sigma_w}\cdot\sqrt{\frac{\hat{I}}{2I_o\gamma}} \qquad (1)$$

where I_o=17kA y is the Alfven current,γ'~2Eacc..

This condition, according to the theoretical description of ref. [1], guarantees the damping of the normalized emittance oscillations (also referred as plasma oscillations), that are caused by slice envelope oscillations produced by mismatches between the space charge correlated forces and the external focusing gradient. The process has been extensively simulated: figures 1 and 2 shows the emittance evolution in the region downstream the gun and from the gun to the booster exit in optimized matching conditions with the linac for a 1nC charge and different pulse shapes

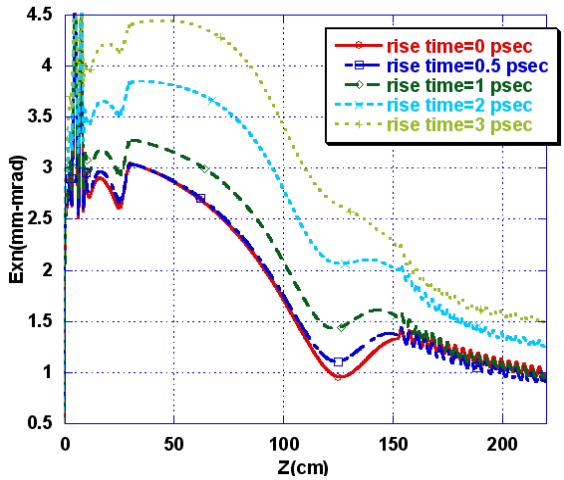

Figure 1: PARMELA simulation of emittance compensation for a 1nC-10ps FWHM pulse and different pulse rise time in the drift downstream the RF gun

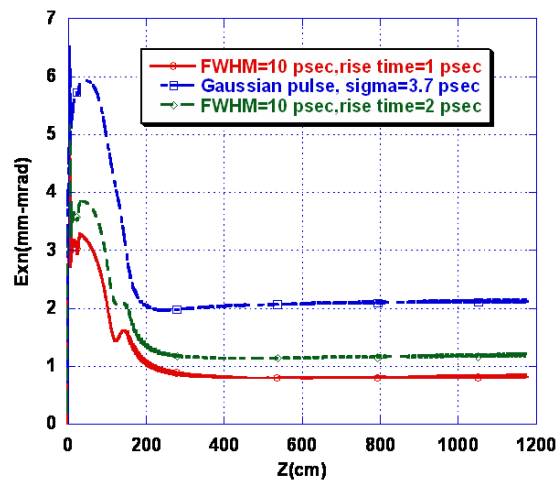

Figure 2: PARMELA simulation of emittance compensation for a 1nC beam and different pulse shapes from the RF gun to the booster exit

In the simulations the "invariant emnvelope" condition is fulfilled and the booster is placed in the position corresponding to the local maximum of the so called "double minimum" emittance oscillation (Ferrario working point [3]) in order to shift the second emittance minimum frozen at low level to the booster exit.

SPACE CHARGE MODELS

The emittance compensation process occours when the beam is in a regime dominated by the space charge, i.e. when the space charge collective force is largely dominant over the emittance pressure. Many numerical codes based on different models have been developed to simulate this regime.

Usually a first scan of initial parameters to identify possible operating points has done by using HOMDYN, a fast semi-analytical code that models the beam as a sequence of slices propagated by a set of envelope equations. It assumes a uniform transverse and longitudinal distribution and neglects the non-linearity in the electromagnetic electric fields. The further exploration of the working points is done by using multiparticle codes as PARMELA (SCHEFF-2D routine) [4] or ASTRA [5] using for the space charge fields the "static" approximation. It consists in calculating the self-fields by solving the Poisson equation for the electrostatic field in the reference frame where the beam may be considered at rest and then transforming the fields back to the laboratory frame where kicks to the particles are applied. In these calculations, assuming a cylindrical symmetry of the beam, a typical number of 20K macro-particles is used. The SCHEFF routine allows to treat also elliptical beams introducing a correction factor on the space charge fields if the ratio between the beam semiaxes doesn't exceed 1.2. If non-homogeneities in the beam spot generated by quantum efficiency variation on photocathode and non-uniformities of laser spot give a significative degradation of the emittance full 3D computations requiring more particles and mesh points than 2D are necessary. In order to evaluate in a quantitative way the beam quality a new parameter, referred as spatial autocorrelation, that is an index of how the uniformities are distributed has been recently introduced [6]: the knowledge of this parameter together with the standard deviation of the spot image allows to give an evaluation of the impact of non-uniformities on the emittance that results higher when the non-homogeneities are more localized. In this case the beam can be modelled by 3D codes such as PARMELA/SPCH3D or the parallel code IMPACT-T [7]. Both codes keep the "static" approximation, collecting and depositing the particles on a three-dimensional grid where the POISSON equation is solved in the beam rest frame. This approximation is good enough until the energy spread is not so high. However in order to handle high energy spreads the IMPACT-T code divides the beam in multiple energy-bins, for each one the space-charge forces are calculated and summed together before being interpolated to individual particles. Another peculiarity of IMPACT-T is the use of an integrated Green function to efficiently and accurately treat beams with large aspect ratio. Recently this last technique has been implemented also in the SPCH3D routine of an upgraded version of PARMELA named TStep [8] reducing the sensitivity to the aspect ratio of the cell dimensions that limited the applicability of the LANL version of PARMELA to aspect ratio not larger than 4.

The "static" approximation is completely disregarded in a different class of three-dimensional codes that are based on the use of retarded potential. Typical examples are TREDI [9] and RETAR [10] codes, that calculate the fields according to the Lienard-Wiechert formalism, taking into account the finite velocity propagation of the signals. This is accomplished by storing the histories of macro-particles and by tracking back in time the source coordinates until a retarded condition is fulfilled, that results in a much time consuming approach. Comparison with other codes [11] that don't take into account this effect show that the finite velocity propagation of the signals doesn't not affect the results in typical photoinjector and that the "retarded" mode is more suitable to describe other classes of problems such as CSR effects in bendings.

EMITTANCE COMPENSATION STUDIES IN SPARC

One of the aims of the SPARC R&D photoinjector facility [12] now under commissioning at INFN-Frascati laboratories is to study the emittance compensation process through accurate comparison between measurements and simulations.

The SPARC facility

The SPARC facility is devoted to the production of a high brightness electron beam driving SASE-FEL experiments at 530 nm and SASE@Seeding HHG tests at 266, 160, 114 nm. It is also the test prototype of the injector of the recently approved SPARX Project [4] for the generation of radiation in the range of 13.5-6 nm and 6-1.5 nm, at 1.5 and 2.4 GeV respectively both in SASE and seeded FEL configurations.The schematic layout is shown in Fig. 3. It consists of a UCLA/SLAC/BNL 1.6 cells S band RF gun with an incorporating metallic cathode operating at a maximum gradient of 120 MV/m followed by a solenoid lens composed of four independently powered coils and three SLAC-type travelling waves accelerating a 1nC-10ps beam with a projected emittance ≤ 2 mm-mrad and a slice emittance ≤ 1 mm-mrad. to 150-200 MeV.

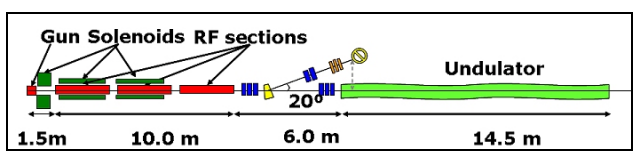

Figure 3: Schematic SPARC layout

The first two accelerating sections are embedded in a solenoid in order to match the beam envelope with the linac and to control the emittance during "velocity bunching" experiments in view of the use of this compression technique for the implementation in SPARX of the hybrid RF-magnetic compression scheme that is one of the peculiarities of the facility.

First SPARC commissioning phase

The first phase of the SPARC commissioning (fig. 4) consisted in characterizing the electron beam in the region downstream the gun by using the movable emittance-meter, a sophisticated diagnostic tool that allowed to measure the evolution of beam size, energy spread, rms transverse emittance and transverse phase space at different locations along the beamline in a range of 1-2.1 m from the cathode. The most relevant experimental results are reported in references [13,14].

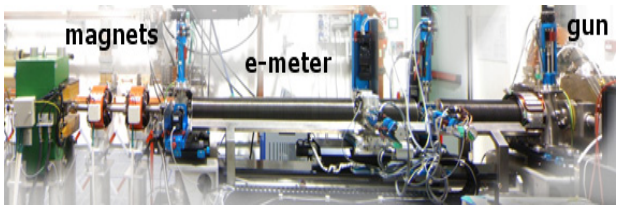

Figure 4: SPARC in the first commissioning phase

In this way it has been possible to study experimentally the emittance compensation process under different operating conditions (variation of pulse shape, charge, gun RF phase) and to perform accurate comparisons between measurements and PARMELA code simulations. The beam model was based for the longitudinal distribution on the cross-correlator measurement of the time profile and for the transverse distribution on the "virtual cathode" image obtained by splitting the laser beam before it enters in the vacuum system.

Some approximations are included in this model: as to the longitudinal distribution the modification of the pulse due to the Schottky effect is not taken into account that can be considered as a second-order effect and, as to the transverse distribution, it is assumed that the laser spot distribution is not strongly modified by disuniformities of the cathode emission. This last approximation was found very good expecially for rms spot sizes less than 400 μm.

The strategy of comparison between measurements and simulations has been done in two steps. The first one was based on the use of an equivalent uniform beam with σ_x and σ_y retrieved from the virtual cathode image and a longitudinal distribution equal to the measured pulse shape. Also due to the reduced level of ellipticity that usually was less than 1.1 it has been possible to use this equivalent beam in some fast 2D runs based on only 20K particles in which the consistency of the main operation parameters with the measured envelope has been checked, by moving the values within some small ranges of uncertainties around the measured value (±1° for the phase, ±5% for the charge and ±1% for the energy). Including these degrees of freedom in simulations is a way to take into account the systematic errors.

The second step of the comparison technique consists in the refinement of computations based on a full 3D model based on a number of particles up to 500K in order to take into account the local disuniformities of the laser spot to compare at the best the simulated and measured emittance. The number of mesh intervals used for these 3D calculations was 32 for the two transverse directions and 64 for the longitudinal direction. The mesh size is automatically adjusted by the code.

A short review of the most relevant results is shown in the plots of figure 5 with the corresponding initial laser spots and pulse shapes reported in figure 6. The emittance oscillations foreseen by the theory and simulations have been observed confirming the reliability of the theoretical and numerical model. In particular Figure 5c refers to the first experimental observation of the "double minimum" emittance oscillation" on which the SPARC working point is based [6]. Figure 7 shows a comparison between the phase spaces retrieved from the measurements and the computed ones in three different z-positions around the relative maximum of the emittance oscillation. A cross-shape is visible due to the fact that under laminar conditions different parts of the bunch reach the space charge dominated waist in different longitudinal positions.

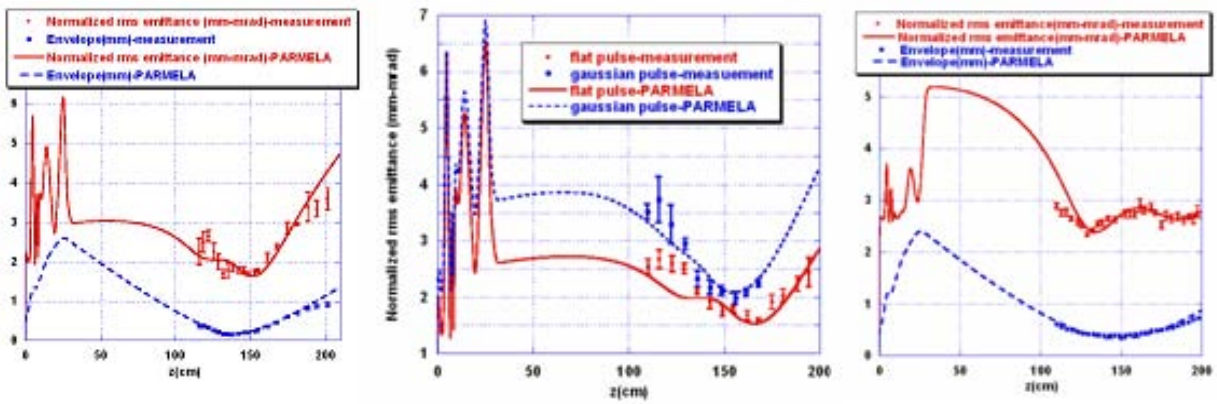

(a) (b) (c)

Figure 5: Emittance-meter measurements and simulation comparison: (a) Emittance and envelope vs z for the highest measured brightness beam (7 10^{13} A/m^2); (b) Emittance evolution comparison between a gaussian and a flat pulse with the same FWHM for a 740 pC beam (c) "Double minimum" emittance oscillation: emittance and envelope vs z.

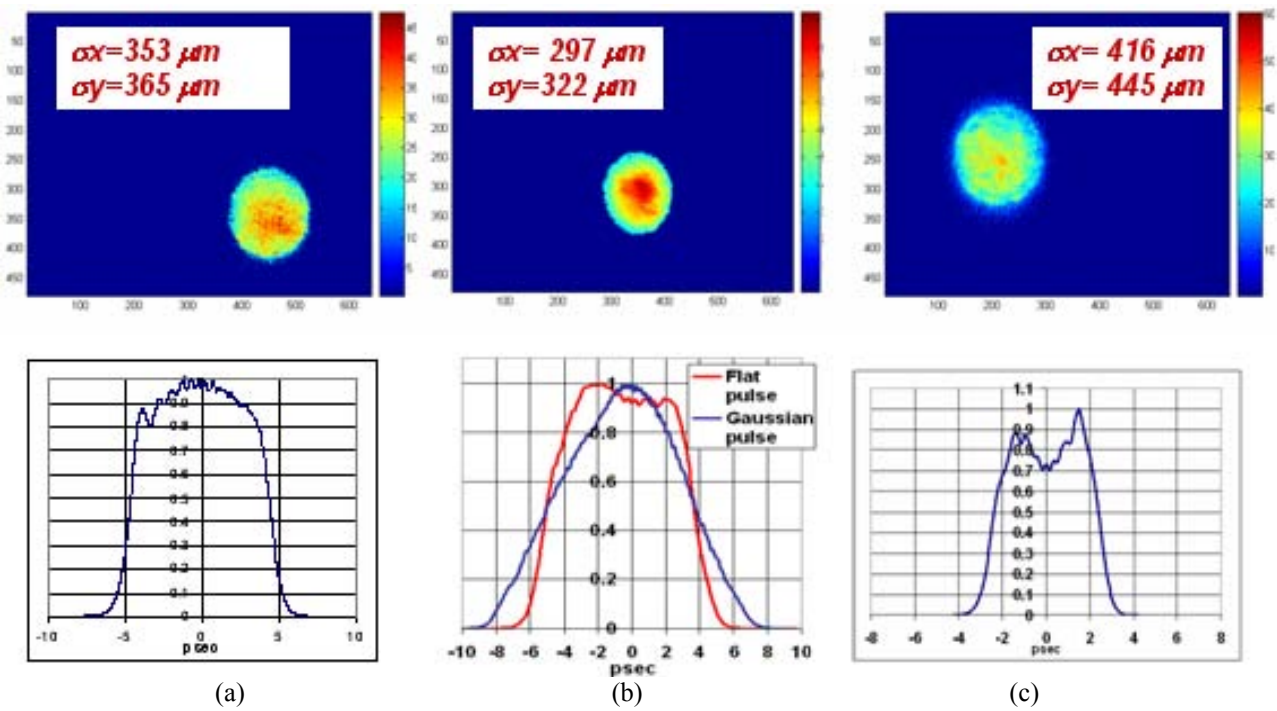

(a) (b) (c)

Figure 6: Virtual cathode spot and pulse shapes coresponding to the plots of figure 5

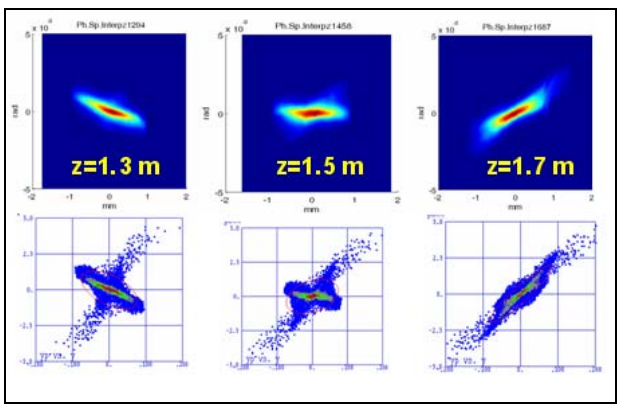

Figure 7: Measured and computed phase spaces in three different z positions in the region of the "double-minimum" emittance oscillation

Figure 8: SPARC in the second commissioning phase

Second SPARC commissioning phase

The second commissioning phase, concerning the beam characterization at full energy, is underway (fig.8). It foresees a detailed analysis of the beam matching with the linac based on the "invariant envelope" criterium and the demonstration of the emittance control in regime of "velocity bunching" in the linac. A poorer performance of the cathode in terms of efficiency, emission uniformity and stability respect to the first phase did not allow to work at the maximum charge and to perform systematic studies of beam optimization. However it has been possible to do some preliminary tests of beam transport up to the exit of the third accelerating structure for checking the diagnostic systems [16] and doing the first comparison with simulations.

Following the experience done in the first phase of the commissioning we firstly looked for the agreement between measurements and fast simulations based on an equivalent uniform beam respect to an envelope measurement. During the transport the spot rms size is measured on four YAG screens: each one of the three first screens is placed at the entrance of the RF structure and the fourth is located at the exit of the linac, where the rms emittance is measured by a quadrupole scan and the bunch length and slice emittance are measured with a high resolution RF deflector [17].

During the first tests an emittance slightly below 2 mm-mrad in the two planes has been obtained with 500pC and a pulse length of 8.5 psec. Figure 9 shows the envelope sampled along the linac compared with a PARMELA simulation. The agreement with simulations is very good, but shows that the transport in the linac is not optimized

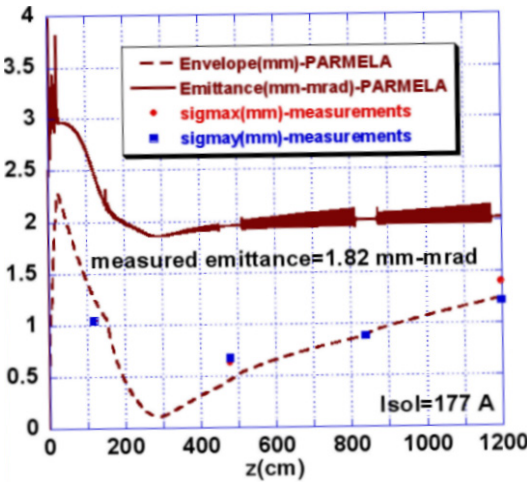

Figure 9: PARMELA simulation of envelope compared with the measured envelopes (red and blue rectangles) an emittance

In fact simulations of a fine magnetic field scan show that some additional improvement in the beam quality are possible as it shown in figures 10 and 11: the solenoid current minimizing the emittance is 185 A (against the value of 177 A used in the measurement) corresponding to a better matching of the beam envelope in the linac, able to decrease the emittance to 1.34 mm-mrad.

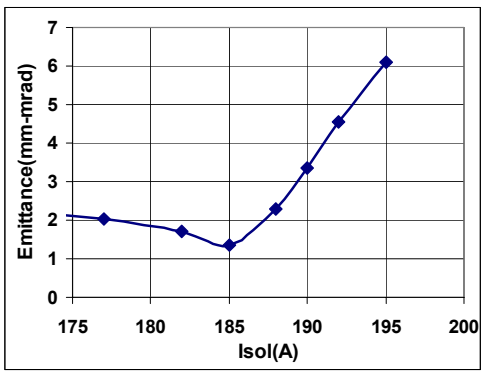

Figure 10: PARMELA simulation: scan of the magnetic field of the gun solenoid

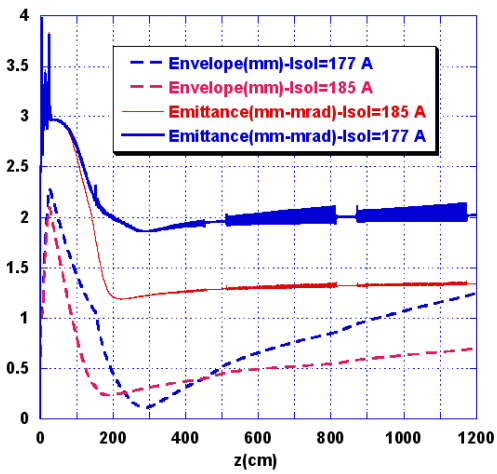

Figure 11: PARMELA simulations: emittance-envelope comparison between the measurement conditions (Isol=177 A) and the optimized maching (Isol=185 A)

Some preliminary tests of beam longitudinal dynamics in regime of "velocity bunching" have been also performed. Figure 12 shows the measured compression factor for a 250 pC beam vs the phase of the first travelling wave section measured by the RF deflector. The reduction of the bunch length from 5 psec to 2.5 psec for a phase range variation of 20 degs is in agreement with PARMELA simulations.

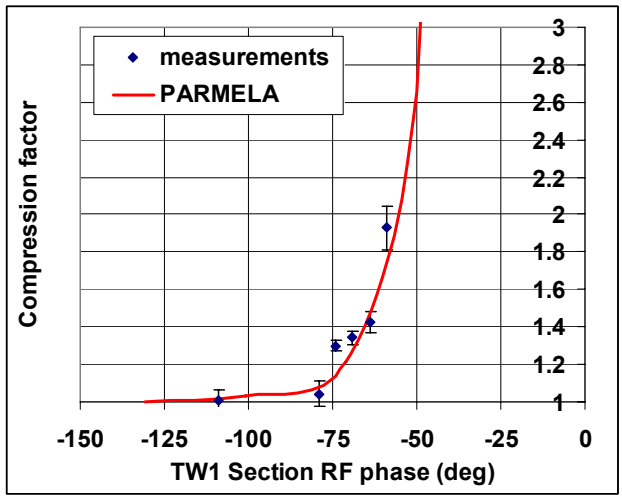

Figure 12: First test of velocity bunching: compression factor vs the phase of the first TW section. Comparison between measurements and simulations

REFERENCES

[1] B. E. Carlsten, NIM A 285, 311-319 (1989)
[2] L. Serafini, J. B. Rosenzweig, Phys. Rev. E 55, 7565-7590 (1997)
[3] M. Ferrario et al., SLAC-PUB-8400, (2000)
[4] L. M. Young, PARMELA, Los Alamos National Laboratory Report LA-UR-96-1835
[5] K. Floetmann, ASTRA http://www.desy.de/~mpyfloASTRA_dokumentation
[6] V. Fusco et al., "Spatial autocorrelation for transverse beam quality characterization", this conference
[7] J. Qiang et al., Phys. Rev. Special Topics – Accel. Beams 9, 044204, (2006)
[8] L. Young, private communication
[9] F. Ciocci et al., Nuclear Instruments & Methods A 393, 434 (1997)
[10] A. Bacci et al, Proceedings of PAC03, p. 3512
[11] C. Limborg et al., Proceedings of PAC03, p. 3548
[12] M. Ferrario et al., "Recent results and Future Perspectives of the SPARC Project", this conference.
[13] L. Palumbo "Status of the SPARX Project", this conference
[14] A. Cianchi et al., PRST-AB, 11, 032801 (2008)
[15] M. Ferrario et al., Phys. Rev. Let. 99, 234801 (2007)
[16] A. Cianchi et al., "Preliminary characterization of the beam properties of the SPARC Photoinjector", this conference
[17] C. Vaccarezza, "Slice emittance measurements at SPARC Photoinjector with a RF deflector", this conference